Synapsin-caveolin-1 Mitigates Cognitive Deficits and Neurodegeneration in PSAPP Mice

Shanshan Wang
UCSD: University of California San Diego https://orcid.org/0000-0001-8249-4291
Joseph Leem
UC San Diego: University of California San Diego
Sonia Podvin
UCSD: University of California San Diego
Vivian Hook
UCSD: University of California San Diego
Natalia Kleschevnikov
UCSD: University of California San Diego
Paul Savchenko
UCSD: University of California San Diego
Mehul Dhanani
UCSD: University of California San Diego
Kimberly Zhou
UCSD: University of California San Diego
Isabella Kelly
UC San Diego: University of California San Diego
Tong Zhang
The Ohio State University
Atsushi Miyanohara
UCSD: University of California San Diego
Alexander Kleschevnikov
UCSD: University of California San Diego
Steve Wagner
UCSD: University of California San Diego
John Trojanowski
University of Pennsylvania
David Roth
UCSD: University of California San Diego
Hemal Patel
UCSD: University of California San Diego
Piyush Patel

UCSD: University of California San Diego

Brian Head (bhead@ucsd.edu)

University of California San Diego, Department of Anesthesiology, VASDHS (9125), 3350 La Jolla Village Drive, San Diego, CA 92161, USA https://orcid.org/0000-0001-9417-5351

Research article

Keywords: Caveolin-1, Membrane lipid raft (MLRs), gene therapy, PSAPP, Alzheimer's Disease, synaptic ultrastructure

Posted Date: September 25th, 2020

DOI: https://doi.org/10.21203/rs.3.rs-79305/v1

Abstract

Background: AD presents with severe neurodegeneration which leads to cognitive deficits and dementia. While many previous approaches focused on targeting amyloid and/or tau, we identified a novel molecular and cellular target that attenuates neurodegeneration in AD which may be exploited as therapeutic targets.

Methods: Using immunoblot, microscopic immunofluorescence and proteomic analysis, the current study revealed that PSAPP transgenic mice exhibit decreased hippocampal caveolin-1 (Cav-1), a membrane/lipid raft (MLR) scaffolding protein that organizes synaptic signaling components. Subcellularly, Cav-1 and full length (fl)-TrkB were significantly decreased in hippocampal MLRs. We thus used viral vector that contains a neuronal-targeted Cav-1 construct using the synapsin promoter (SynCav1) to re-express Cav-1 in PSAPP mice. Effects of SynCav1 on cognition function, hippocampal neuron morphology and ultrastructure were examined at 9 (presymptomatic stage) and 11 month (symptomatic stage) respectively.

Results: While PSAPP mice showed significant learning and memory deficits at 9 and 11 months, PSAPP mice that received hippocampal SynCav1 (PSAPP-SynCav1) maintained normal learning and memory at 9 and 11 months respectively. Furthermore, PSAPP-SynCav1 mice showed preserved hippocampal MLR-localized fl-TrkB, synaptic ultrastructure, dendritic arborization and axonal myelin content, all of which occurred independent of reducing amyloid deposit and astrogliosis.

Conclusions: While transgenic PSAPP mice exhibit decreased hippocampal expression of the MLR scaffolding protein Cav-1 in the early stage of disease, SynCav1 mitigated neuropathology and cognitive deficits in PSAPP mice. Irrespective of amyloid, our approach targeted neuronal degeneration pathways that may be downstream of amyloid species and/or tau in AD but also other forms of neurodegeneration of different or unknown etiology.

Full Text

This preprint is available for download as a PDF.

Figures

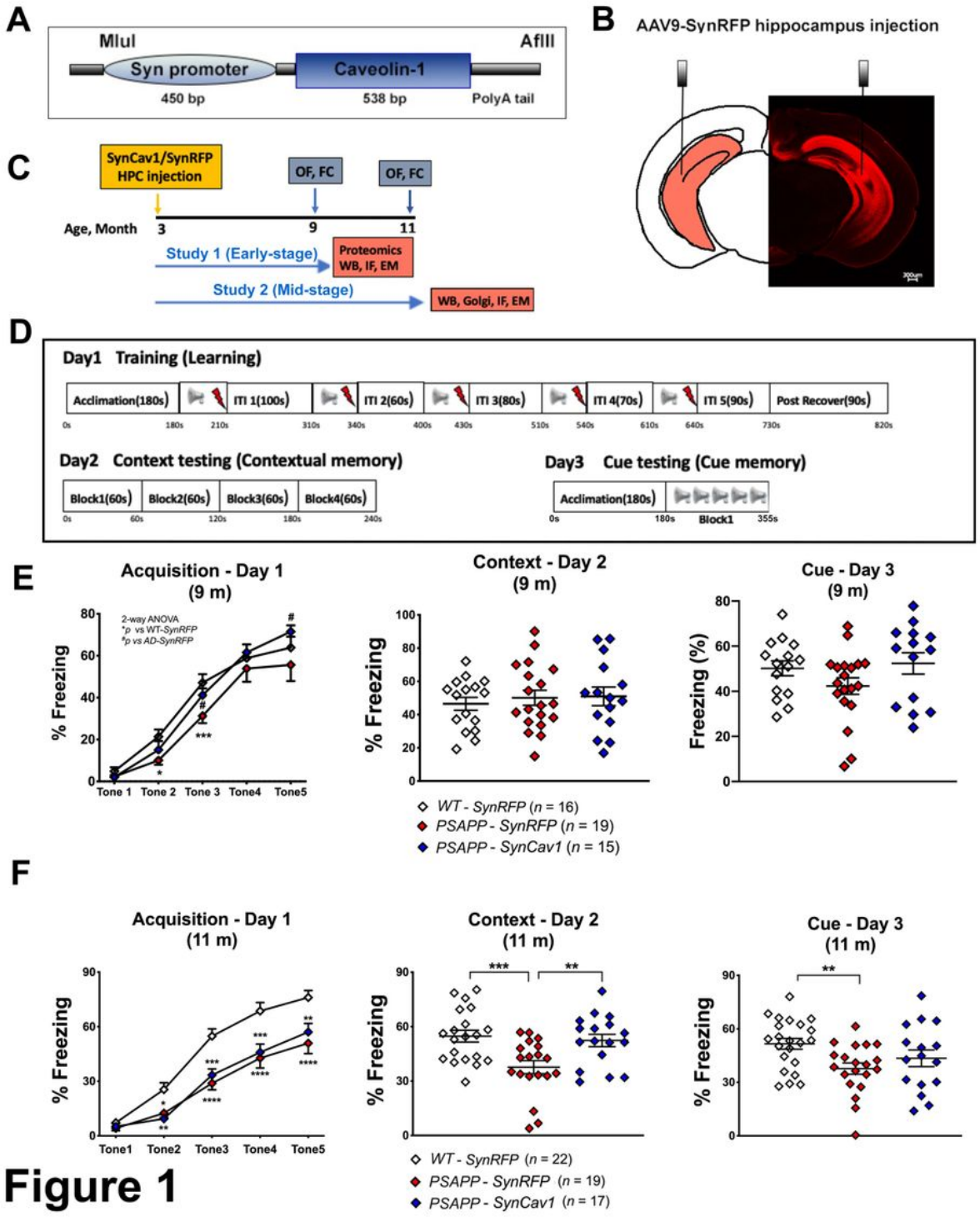

Figure 1

Figure 1

SynCav1 gene delivery preserves learning and memory in 9 and 11 month-old PSAPP (APPSwePS1d9) mice. (A) Viral structure of AAV9-SynCav1. (B) Illustration (left) and microscopy of hippocampal RFP. (C) Schematic of experimental design in WT and PSAPP (APPSwePS1d9) mice. Blue arrows and rectangular boxes indicate open field and fear conditioning tests for separate 9 and 11 m cohorts; orange arrows and rectangular boxes indicate postmortem biochemical assays. (D) Schematic of fear conditioning protocol.

Fear conditioning test showed that at 9 m (E), PSAPP-SynRFP mice only exhibited reduction in fear learning acquisition on day 1 compared to WT-SynRFP with normal contextual memory recall on day 2. At 11 m (F), both PSAPP groups exhibited a significant reduction in learning on day 1 compared to WT-SynRFP. On day 2, PSAPP-SynRFP mice exhibited a significant reduction in contextual memory recall versus WT-SynRFP while PSAPP-SynCav1 exhibited normal contextual memory recall. Data are presented as percent (%) freezing mean ± SEM. Data were analyzed using two-way analysis of variance (ANOVA) followed by Fisher's LSD multiple comparisons tests (Day 1) or One-way ANOVA (Day 2 and 3). n = 14-19 animals per group for 9 m; n = 17-22 per group for 11 m. Significance was assumed when $p < 0.05$. *$p < 0.05$, **$p < 0.01$, ***$p < 0.001$, ****$p < 0.0001$.

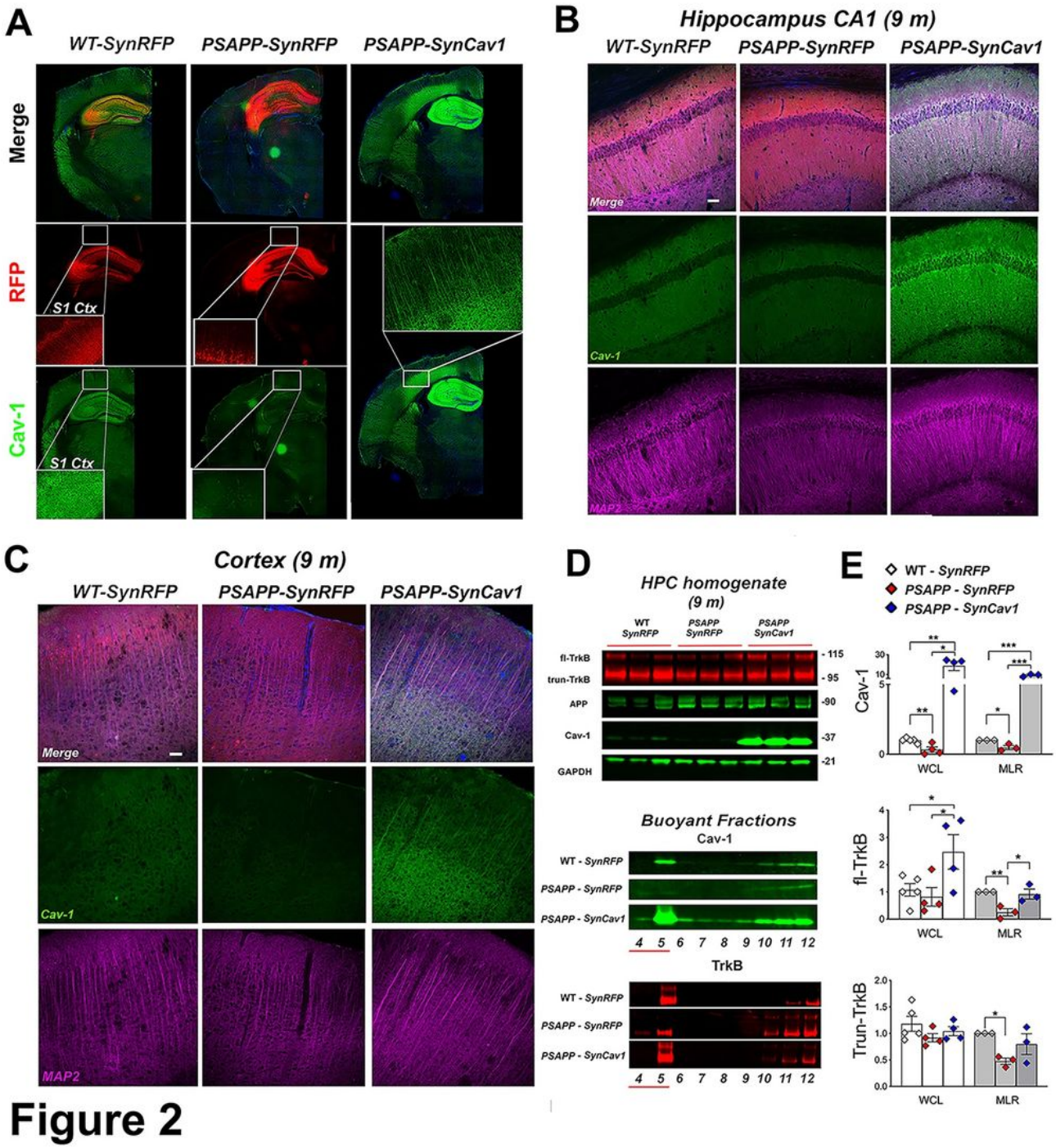

Figure 2

Figure 2

SynCav1 gene delivery preserves hippocampal MLR-localized Cav-1 and fl-TrkB expression in 9 m PSAPP mice. (A) Immunofluorescence microscopy revealed significantly decreased Cav-1 in 9 m PSAPP mice hippocampus. (B-C) Co-staining for Cav-1 and dendritic marker MAP2 showed that SynCav1 gene delivery preserved MAP2 expression in dendritic processes in the hippocampal CA1 subfields CA and cortex in 9-month old PSAPP mice. Scale bar = 50 um. IB (D-E) of 9 m hippocampal homogenates and buoyant

fractions (i.e., MLRs) revealed decreased Cav-1 and full-length TrkB (fl-TrkB) expression in PSAPPSynRFP mice vs WT-SynRFP mice. SynCav1 preserved hippocampal MLR localized fl-TrkB expression in PSAPP mice. Fractions were generated from equal protein (0.5 ug/ul). Data present as mean ± SEM, n = 3-4 animals per group. Data were analyzed using t test (Cav-1 expression) or One-way ANOVA (TrkB). Significance was assumed when $p < 0.05$. *$p < 0.05$, **$p < 0.01$, ***$p < 0.001$.

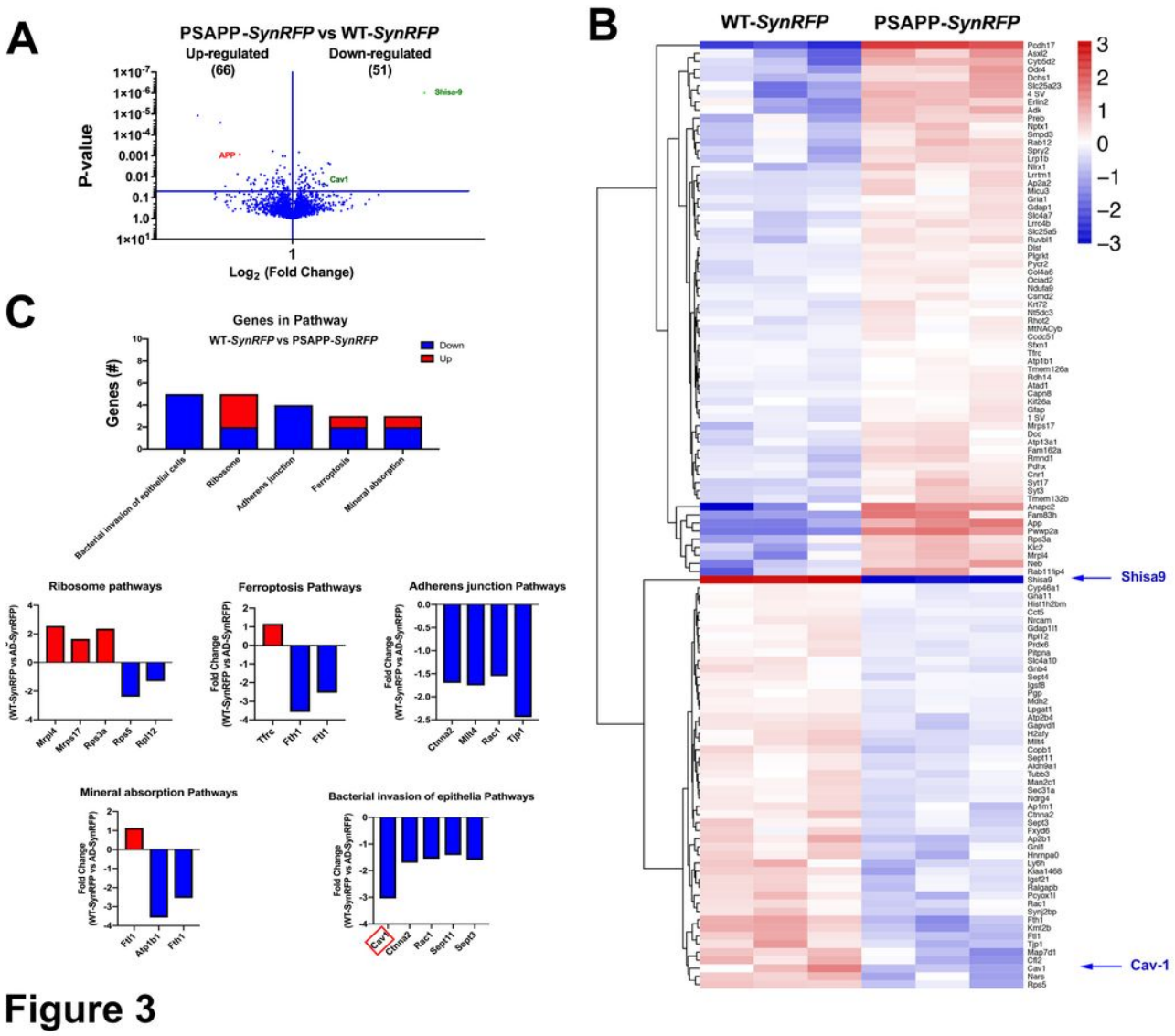

Figure 3

Figure 3

Proteomics reveals altered MLR-associated proteins in PSAPP-SynRFP mice at 9 m. (A) Volcano plot of 9 m MLRs between WT-SynRFP and PSAPP-SynRFP identified 117 genes that were differentially expressed (65 upregulated and 52 down regulated). (B) Mean expression differences of significantly regulated proteins were evaluated by Euclidean hierarchical clustering. (C) Gene ontology (GO) functional enrichment using STRING-db. Clustering revealed that Cav-1 was among the significantly downregulated in MLRs from PSAPP-SynRFP hippocampi. All significantly regulated quantifiable protein groups together evaluated for significant gene ontology (GO) functional enrichment using STRING-db (www.string-db.org). The most significant GO terms identified were Bacterial Invasion of Epithelial Cells, Ribosome,

Ferroptosis, Mineral Absorption, and Adherens Junction. All proteins in this GO term and Adherens Junction were downregulated in PSAPP-SynRFP versus WT-SynRFP. The significantly different expression levels between comparison groups were determined by two-tailed Student t test, n = 3 animals per group. Significance was assumed when *p < 0.05.

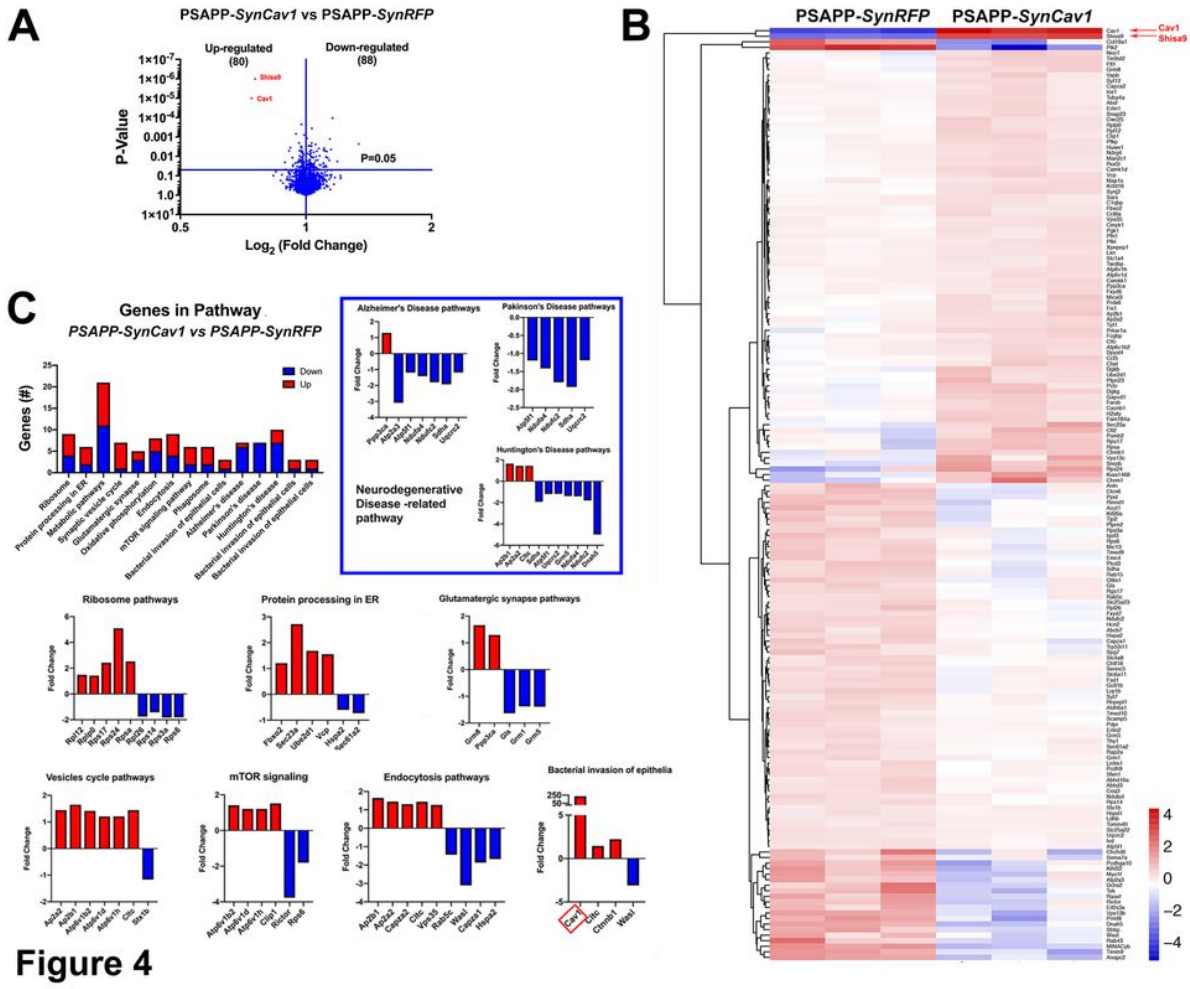

Figure 4

Figure 4

Proteomics reveals that SynCav1 decreases expression of neurodegenerative genes in MLR fractions from 9 m PSAPP mice. (A) Volcano plot of 9 m MLRs between PSAPP-SynRFP and PSAPP-SynCav1 identified 168 genes that were differentially expressed (80 upregulated and 88 down regulated). (B) Mean expression differences of significantly regulated proteins were evaluated by Euclidean hierarchical clustering. Cav-1 was the most upregulated protein (log2 = 7.8) due to its overexpression with SynCav1. Notably, several downregulated proteins in MLRs from PSAPP-SynRFP (shisa9, ap2b1, cofilin-2, cct-5, FXYD, Kiaa1468, MAN2C1, NDRG4, synaptojanin2, Prdx6) were significantly upregulated in MLRs from PSAPP-SynCav1. Gene ontology (GO) functional enrichment using STRING-db demonstrated that several genes implicated in neurodegenerative disease pathways (e.g., AD, Parkinson's, Huntington's) were significantly down regulated in MLRs from PSAPP-SynCav1 when compared to PSAPP-SynRFP (C). Red

rectangular box in Bacterial Invasion of Epithelia Pathways in C denotes increased Cav-1. The significantly different expression levels between comparison groups were determined by two-tailed Student t test, n = 3 animals per group. Significance was assumed when *p < 0.05.

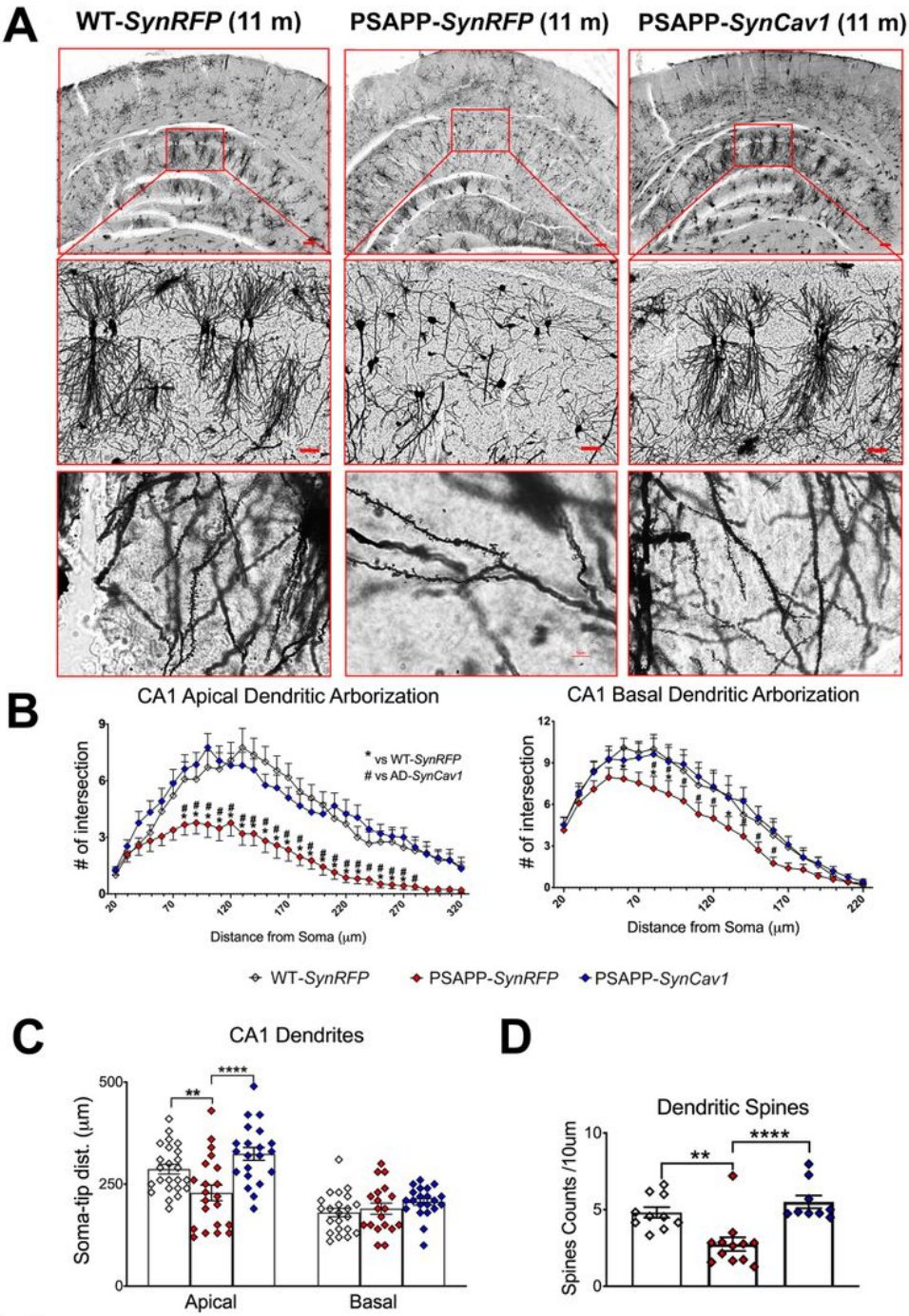

Figure 5

Figure 5

SynCav1 gene delivery preserves dendritic arborization in CA1 hippocampal neurons from 11 m PSAPP mice. Golgi- Cox images of cornu ammonis (CA1) pyramidal neurons (Top row scale bar = 200 um;

middle row images scale bar = 50 um) (A). Quantification revealed a significant reduction in CA1 apical and basal dendritic arborization in PSAPP-SynRFP mice compared to WT-SynRFP and PSAPP-SynCav1 mice. AD-SynCav1 showed preserved apical dendritic arborization from 70 to 280 um distance from the soma and basal dendritic arborization from 80 to 150 um distance (B). PSAPP-SynRFP mice also showed decreased apical dendrite soma to tip distance, which was preserved by SynCav1 (C). No difference in basal dendrite soma to tip distance (C). Further analysis revealed decreased CA1 spine number in PSAPP-SynRFP mice and preserved dendritic spines in PSAPP-SynCav1 (D). Data are presented as mean ± SEM, n = 3 animals in each group consisting of 8-12 neurons from each animal. Data were analyzed using One-way ANOVA. Significance was assumed when $p < 0.05$. *$p < 0.05$, **$p < 0.01$, ***$p < 0.001$.

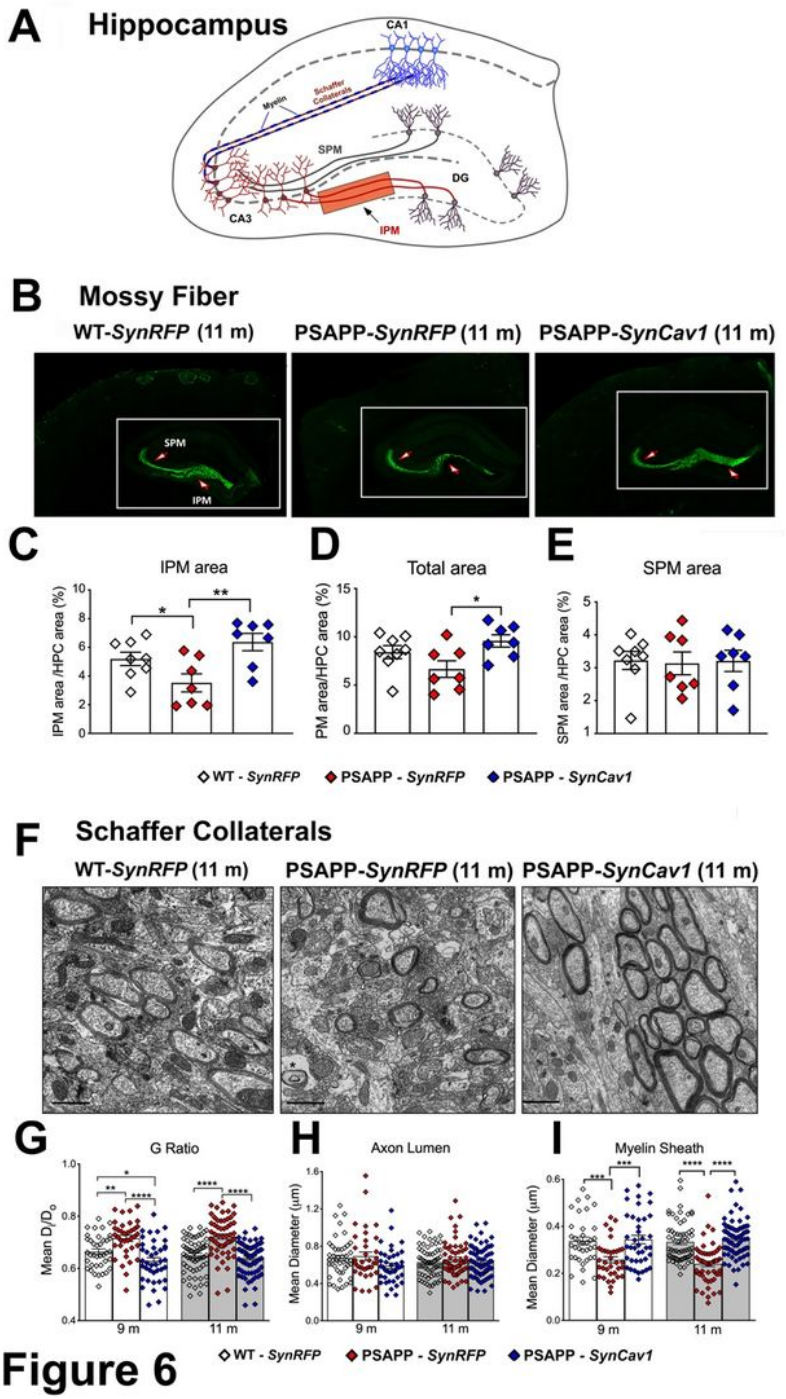

Figure 6

Figure 6

SynCav1 gene delivery preserves axonal structure and myelin content in the hippocampus of 9 m and 11 m PSAPP mice. (A) Illustration of hippocampal pathways. (B) Infrapyramidal and suprapyramidal mossy fiber structures at 11 m (n = 3-4 animals per group consisting of 2-3 images per animal). PSAPP-SynRFP mice exhibited significantly reduced IPM area (C, D) compared to WTSynRFP, while the PSAPP-SynCav1 group showed significantly greater IPM area compared to PSAPP-SynRFP, with no significant difference

in SPM area detected (E). (F) EM images of myelinated CA3 Schaffer collateral axons. G-ratio analysis of CA3 Schaffer collateral axons (axon lumen diameter (Di)/fiber (axon lumen + myelin) diameter (Do)) at 9 m and 11m revealed that the G-ratio was increased in PSAPP-SynRFP mice versus WT-SynRFP (G), an alteration due to reduced myelin sheath diameter (I), rather than increased axon lumen diameter (H). PSAPP-SynCav1 mice exhibited significantly decreased G-ratio compare to PSAPP-SynRFP due to increased myelin sheath diameter. Micrographs were captured at 11000x Magnification, scale bar = 500 nm. Data are presented as mean ± SEM, n = 3-6 animals per group consisting of 10 electron micrographs images per animal. Data were analyzed using One-way ANOVA within each time point. Significance was assumed when $p < 0.05$. *$p < 0.05$, **$p < 0.01$, ***$p < 0.001$, ****$p < 0.0001$.

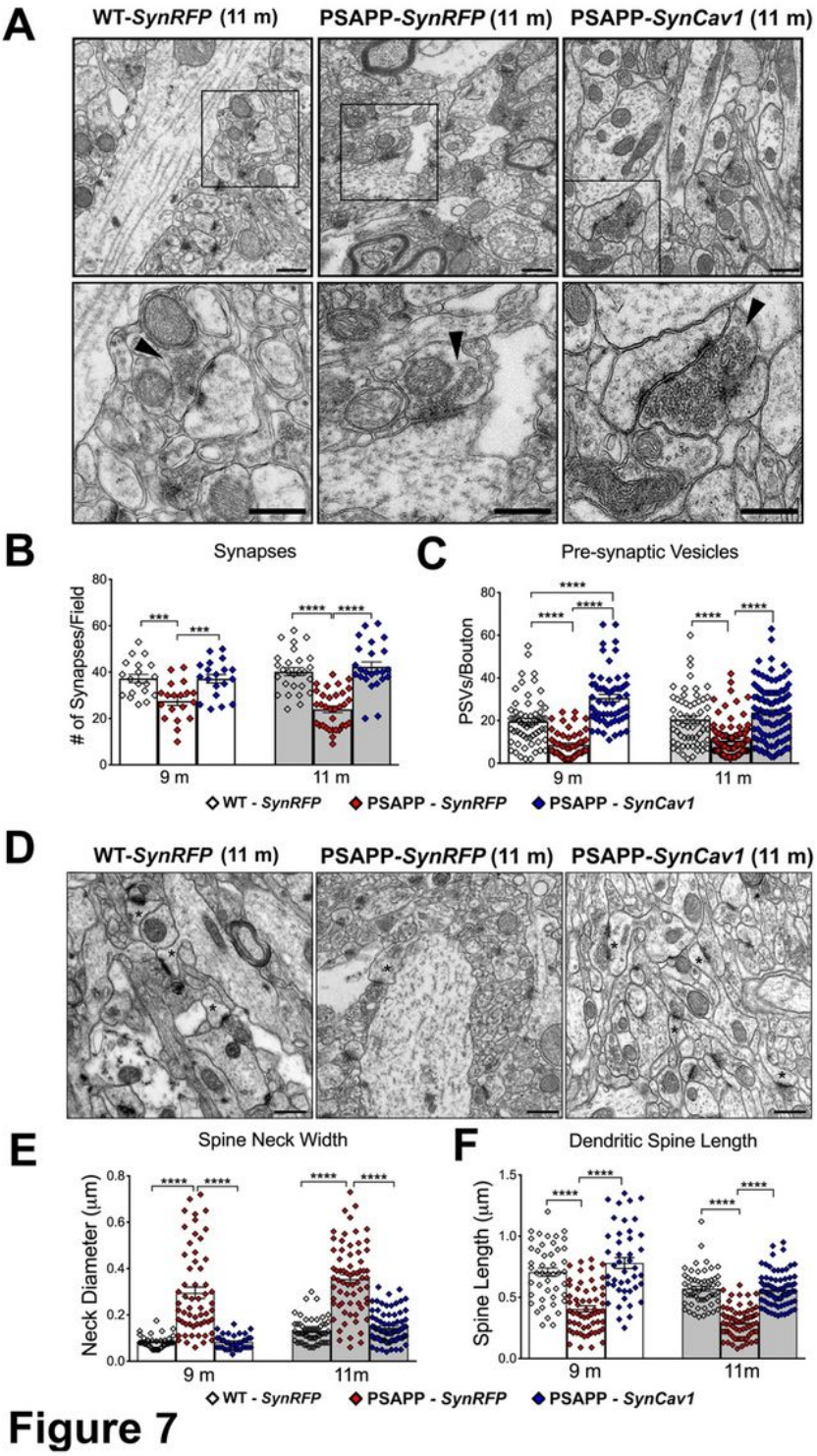

Figure 7

Figure 7

SynCav1 gene delivery preserves synaptic ultrastructure and dendritic spine morphology in the hippocampus of 9 m and 11 m PSAPP mice. EM images (A) and quantitation of total type I asymmetric synapses (B) and presynaptic vesicles (PSVs)/axonal bouton (C) in hippocampal CA1 distal apical dendrites in the stratum radiatum. PSAPP-SynRFP mice demonstrated a significant reduction in total type I excitatory asymmetric synapses and total number of pre-synaptic vesicles (PSVs)/bouton. In contrast,

PSAPPSynCav1 mice showed a significant increase in both total synapses and total number of PSVs/bouton when compared to PSAPPSynRFP and WT-SynRFP. Top micrographs represent 4800x Magnification, scale bar = 1 um; bottom micrographs represent 11000x Magnification, scale bar = 500 nm. Black arrow heads denote asymmetric type I synapses. EM images (D) and quantitation of dendritic spine neck width (E), length (F) showed that PSAPP-SynRFP mice exhibited altered dendritic spine morphology (i.e., morestubby and less mushroom-like spines) with significantly increased neck diameter and reduced spine length compare to WT-SynRFP. PSAPP-SynCav1 mice showed preserved neck diameter and increased spine length when compared to PSAPP-SynRFP. Same trend was observed at 11 month age. Micrographs represents 11000x Magnification, scale bar = 500 nm. Data are presented as mean ± SEM, n = 3-6 animals per group consisting of 10 electron micrographs per animal. Data were analyzed using One-way ANOVA within each time point. Significance was assumed when $p < 0.05$. *$p < 0.05$, **$p < 0.01$, ***$p < 0.001$, ****$p < 0.0001$.

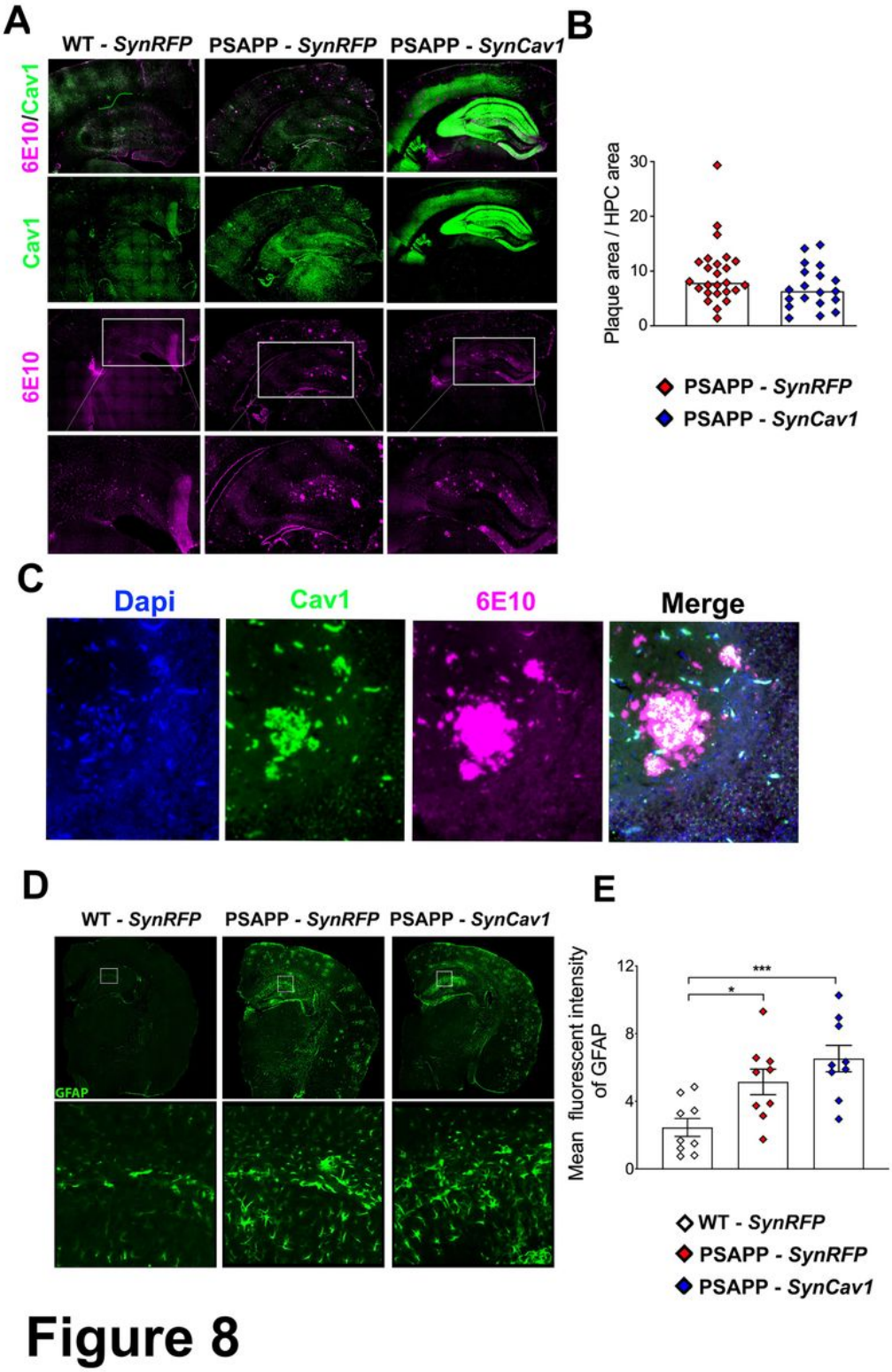

Figure 8

Figure 8

SynCav1 did not mitigate hippocampal amyloid plaque deposits nor astrogliosis in 11 m PSAPP mice. (A-B) Cav1/6E10 dual staining of 11 month PSAPP mouse and hippocampi 6E10-positive amyloid deposits quantitation at 11 m. (C) Cav1/6E10 dual staining of 11 month PSAPP mouse hippocampus sub-region showed a colocalization of Cav1 with amyloid plaque, cell nuclei were counterstained with DAPI (blue). (D-E) GFAP (astrocytes) staining with hippocampi quantitation at 11 m. Data were analyzed using

Student t test for 6E10 analysis, n = 5-6 animals per group. Data were analyzed using one-way ANOVA for GFAP analysis, n = 3-4 animals per group. Significance was assumed when *p < 0.05.

Supplementary Files

This is a list of supplementary files associated with this preprint. Click to download.

- supplement5.pdf